IEEE Access
Multidisciplinary | Rapid Review | Open Access Journal

Received September 7, 2019, accepted September 18, 2019, date of publication September 24, 2019,
date of current version October 15, 2019.

Digital Object Identifier 10.1109/ACCESS.2019.2943454

Rapid Detection of Rice Disease Based on FCM-KM and Faster R-CNN Fusion

GUOXIONG ZHOU, WENZHUO ZHANG, AIBIN CHEN, MINGFANG HE, AND XUESHUO MA
College of Computer and Information Engineering, Central South University of Forestry and Technology, Changsha 410004, China
Corresponding authors: Guoxiong Zhou (51840157@qq.com) and Aibin Chen (5708111@qq.com)

This work was supported by the National Natural Science Foundation of China under Grant 61703441.

ABSTRACT In this paper, a method for detecting rapid rice disease based on FCM-KM and Faster R-CNN fusion is proposed to address various problems with the rice disease images, such as noise, blurred image edge, large background interference and low detection accuracy. Firstly, the method uses a two-dimensional filtering mask combined with a weighted multilevel median filter (2DFM-AMMF) for noise reduction, and uses a faster two-dimensional Otsu threshold segmentation algorithm (Faster 2D-Otsu) to reduce the interference of complex background with the detection of target blade in the image. Then the dynamic population firefly algorithm based on the chaos theory as well as the maximum and minimum distance algorithm is applied for optimization of the K-Means clustering algorithm (FCM-KM) to determine the optimal clustering class k value while addressing the tendency of the algorithm to fall into the local optimum problem. Combined with the R-CNN algorithm for the identification of rice diseases, FCM-KM analysis is conducted to determine the different sizes of the Faster R-CNN target frame. As revealed by the application results of 3010 images, the accuracy and time required for detection of rice blast, bacterial blight and blight were 96.71%/0.65s, 97.53%/0.82s and 98.26%/0.53s, respectively, indicating clearly that the method is more capable of detecting rice diseases and improving the identification accuracy of Faster R-CNN algorithm, while reducing the time required for identification.

INDEX TERMS Chaos theory, faster R-CNN, firefly algorithm, Otsu threshold segmentation, K-means clustering algorithm, rice disease detection, weighted multistage median filter.

I. INTRODUCTION

As one of world's major food crops, rice is stable in production, which is related to agricultural security, social stability and national development. Nevertheless, rice diseases have occurred frequently in recent years, causing serious losses in rice production. Rice diseases are mainly the rice blast, bacterial blight, sheath blight, and symptoms characterized by texture, the color and the shape, which are typical of rapid occurrence and easy infection [1]–[3]. At present, the identification of rice diseases is mainly through artificial identification, querying rice diseases maps and automated detection. Conventional manual identification is inefficient, time-consuming and costly. Although the operation of the diseases map is simple, some diseases with high similarity are easy to be misunderstood. The existing computer-based detection of rice diseases is affected by diseases. Considering the large environmental impact, slow detection speed, and low accuracy, it has not been widely applied. In this case, it is of great significance to make rapid and accurate judgments on rice diseases.

The rice diseases are concentrated in leaves, for which the diagnosis of leaves can guide the growers on whether to spray the crops. In the field of science, great progress has been made in identifying plant diseases by identifying leaf characteristics [4]–[9]. In literature [8], the CNN method is used to identify the Helminthosporium leaf spot of wheat, with the final accuracy and standard error being 91.43% and 0.83, respectively. In literature [10], we use a combination of two improved deep convolutional neural network models GoogLeNet and Cifar10 to identify corn leaf disease, and the average accuracy can reach 98.9% and 98.8%, respectively. In literature [11], the clustering algorithm and the supervised classification algorithm are used to perform lesion image segmentation, extract the feature image, and then normalize and select the feature. By applying the

The associate editor coordinating the review of this manuscript and approving it for publication was Moayad Aloqaily.

pattern recognition method to establish the disease recognition model, accuracy can be ensured in identifying alfalfa leaf disease, with the rate being up to 97.64%. In respect to rice diseases detection [4], [12]–[20], in literature [4], the image was segmented with the entropy-based bipolar threshold method after its brightness and contrast were enhanced. Subsequently, the boundary of the diseased part was detected with the 8-connectivy method. Finally, based on the SOM neural network, the infected part of the leaf was classified. The method developed in this system is used to achieve image processing and soft computing for various diseased rice plants. But the recognition accuracy on the four data sets was 82% on average, which means that it still needs further improvement. In [12], image processing and machine learning techniques were used to screen seedlings with rickets in a non-destructive manner, and SVM classifiers were developed with the help of genetic algorithms in order to optimize feature selection and model parameters; The overall accuracy of the SVM classifiers which were used to distinguish healthy seedlings and infected ones is 87.9%. However, in light of that different varieties may have different symptoms, the method should be examined when used in other varieties or diseases, which indicates that this method has certain limitations. Literature [13] proposed a rice disease identification method (CNNs) based on deep convolutional neural network. Under the 10-fold cross-validation strategy, it was found that the average recognition rate of 10 common rice diseases was 95.48%. Literature [14] proposes a new stacked CNN architecture that uses two-stage training to significantly reduce the size of the model while maintaining high classification accuracy. Based on our experimental results, it was shown that compared to VGG16, by using stacked CNN, the test accuracy reached 95% while the model size was reduced by 98%. This CNN architecture with efficient memory can facilitate the detection and identification of rice diseases based on mobile application development. In [15], the gray level co-occurrence matrix (GLCM) and the color moment of the leaf lesion area were applied for extraction from the diseased and unaffected leaf images to produce a 21-D feature vector and related features and remove redundant features were selected with the feature selection method based on genetic algorithm to generate 14-D feature vectors so as to reduce complexity. Then, classification was conducted by using artificial neural network (ANN) and support vector machine (SVM). Finally, the classification accuracy of the algorithm reached 92.5% through SVM, and 87.5% through ANN. This is an innovative method, but further optimization is necessary if its accuracy of identification needs to be increased. In literature [16], a stochastic gradient descent algorithm (SGD) was proposed to optimize the GoogLeNet model. In addition, in order to prevent the model from overfitting and improving its generalization performance, two data enhancement strategies of randomly discarding one band image and random panning average spectral image brightness were also proposed in the literature. After testing, it was shown that the highest accuracy of the prediction of the disease on the epidermis was 92.0%. However, neither the extraction of high-level abstract features layer by layer in the band dimension nor the band details information was not taken into full consideration or fully used, so there is still a lot of room for improvement in the accuracy.

Relative to other crops such as corn and tomato, there are relatively few studies on the identification of rice diseases. Thus, the technical level of rice diseases detection needs to be improved. Faster R-CNN [21] was proposed by the Ross Girshick team in 2015. Because of its fast speed and high precision, it is suitable for the detection of rice diseases. However, the traditional Faster R-CNN algorithm shows a tendency to generates a large number of bounding boxes, and the speed and accuracy of detection are less than satisfactory, for which there is a necessity to make improvement to the bounding box. The K-Means clustering algorithm (FCM-KM algorithm) optimized by applying the dynamic population firefly algorithm which is improved by chaos theory and maximum and minimum distance algorithm helps address the problem arising from setting the k value of clustering category and overcome the drawbacks of susceptibility to falling into local optimum. Besides, it exhibits the desirable advantage of fast convergence. Therefore, a rapid rice disease detection method based on FCM-KM and Faster R-CNN fusion is proposed in this paper. The FCM-KM algorithm is applied to re-set the bounding box size in Faster R-CNN for the convergence to be accelerated. The accuracy and time of detection of rice blast, bacterial blight and blight were 96.71%/0.65s, 97.53%/0.82s and 98.26%/0.53s, respectively. The results show that this method can better detect rice diseases.

II. RICE DISEASE PERFORMANCE AND RESEARCH STATUS

The main types of rice diseases are the rice blast, bacterial blight, and sheath blight. The rice blast is divided into the nursery, the leaf hopper and ear mites. The main disease of the nursery is that the color of leaves of the rice is gradually deeper and finally becomes brown. The main symptom of the leafhopper is that the shape of leaves is a fusiform or elliptical lesion, while that of the ear is the blackening of the ear of the rice, and that of bacterial blight is that spots form on the edge of the rice leaves in initial period, and then the spots following the leaves become white and then gray and wither. The incidence of sheath blight in the south is relatively high, and its occurrence is more related to climate. The general symptom is that green spots appear on the leaf sheath of the rice plant near the water surface and become larger as the disease progresses, and in the end, a grayish white spot bounded by the brown. In summary, rice diseases are chiefly characterized by texture, the color and the shape.

This paper proposes a method for identifying common diseases of rice, and its structure is shown in Figure 1. Firstly, by collecting pictures of diseases, the image is denoised by a two-dimensional filtering mask combined with an weighted multilevel median filter(2DFM-AMMF); then, the Faster

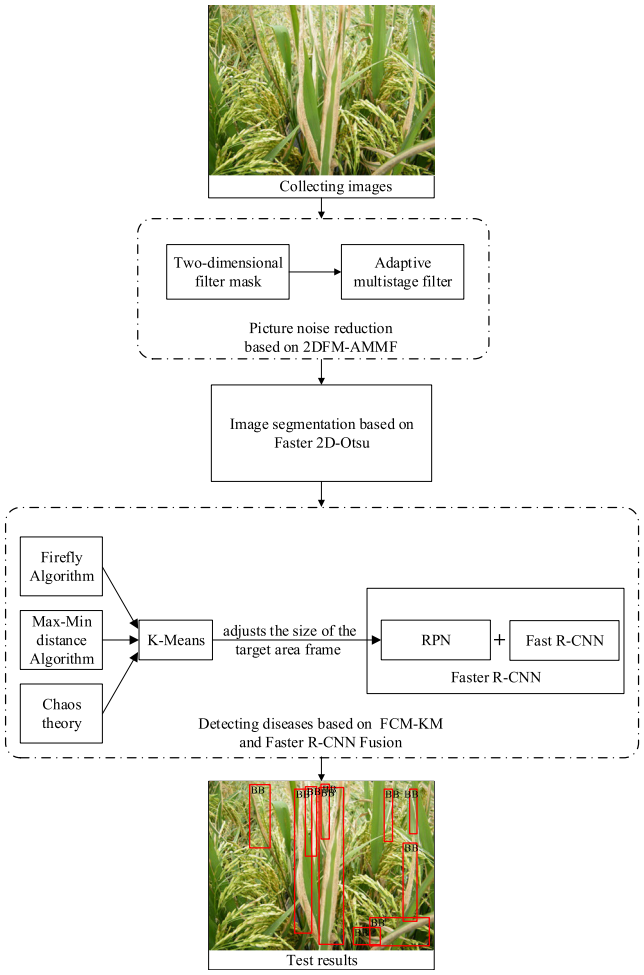

FIGURE 1. Rice disease identification structure.

2D-Otsu is used to segment the noise-reduced image for extraction of the target leaf lesion from the image. Finally, the rapid rice disease detection method based on FCM-KM and Faster R-CNN was applied to extract rice disease characteristics and classify pests and diseases in the segmented pictures, from which the results of rice disease detection are obtained. Among them, the 2DFM-AMMF algorithm is a weighted multilevel median filter in combination with a two-dimensional filtering mask. The basic procedure of the Faster 2D-Otsu algorithm to segment the image is as follows. Firstly, the initial threshold range is calculated. Secondly, the most Good threshold is obtained. Finally, the optimal threshold is applied to segment the rice disease picture. FCM-KM is integrated with Faster R-CNN, that is, the clustering category value K obtained through FCM-KM clustering and its clustering center are taken as input of the Faster R-CNN algorithm to replace the aspect ratio of the original candidate frame, thus changing the size of frame for the target area.

III. MATERIALS AND METHODS

A. GRAPHIC GATHERING

In this text, the picture data of rice diseases are collected from the high-standard rice experimental field of the Hunan Rice Research Institute, and the camera model was Canon EOS R, and the picture pixel was 2400 ∗ 1600. For each image, the sub-image containing the lesion is first obtained by manual cropping, and then the image with too low brightness and blurred image is discarded, and the number of images is expanded by adjusting the angle and appropriately cutting. In the end, a database of three types of rice diseases was compiled, as listed in Table 1, for a total of 3010 images.

TABLE 1. The number and the proportion of diseases in the rice diseases.

Type	Amount	Proportion
Rice blast	1002	33.29%
Bacterial blight	990	32.89%
Sheath blight	1080	33.82%
Total	7448	100%

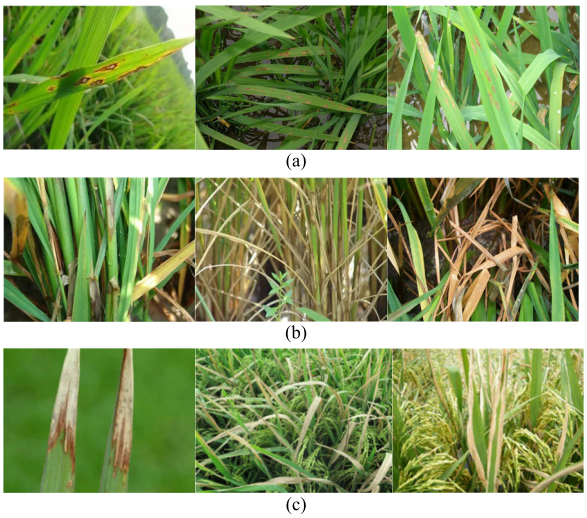

FIGURE 2. Part of the picture of rice diseases: (a) Picture of rice blast. (b)Picture of sheath blight. (c) Picture of bacterial blight.

The picture of the rice disease database is as follows:

Fig. 3 shows some of the images expanded by rotation, cropping, etc.:

B. GE PREPROCESSING BASED ON 2DFM-AMMF

1) WEIGHTED MULTILEVEL MEDIAN FILTERING ALGORITHM

In the process of obtaining and spreading rice diseases, the quality tends to decrease due to external noise interference. The segmentation and feature extraction of noise-containing images may make it unlikely for some disease features to be extracted, which could possibly further affect the accuracy of detection, so it is necessary to reduce the noise [22]. Median filtering is a nonlinear filtering method proposed by Tukey in the early 1970s. The method is simple to operate; it is easy to remove outliers and line noise; it can eliminate binary noise; effectively suppress interference pulses and point noise. The multilevel median filtering proposed later can better maintain the edge and details of the rice disease map, but it is weak noise suppression. Although the

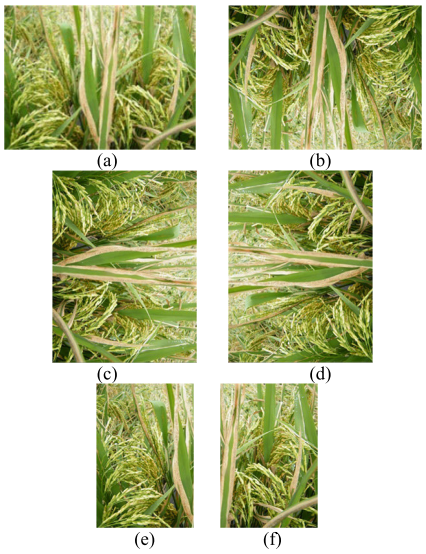

FIGURE 3. Pictures cropped with the angle adjusted: (a) Original image. (b) Rotate 180°clockwise. (c) Rotate 90°clockwise. (d) Rotate 270°clockwise. (e), (f) Crop 1.

multilevel median filter can is capable of improve improving the noise suppression ability after weighting, it is difficult to operate as its noise reduction effect depends on the size and shape of the filter window [5]. Therefore, in this paper, proposes a 2DFM-AMMF based noise reduction method is proposed, which features the adds addition of a two-dimensional filtering mask based on the weighted multilevel median filtering. In this case, so that the size and shape of the filtering window are determined by the image information, thereby reducing the chance of useful edge information being eliminated by the weighted multilevel mean value filter.

The weighted multistage median filter is a filtering method that combines a multilevel median filter and an average weighting algorithm. Let $X\ (i,\ j)$ be the sequence of digital images of rice diseases and W be a square filter window whose center is at (i, j) and size is $L = 2\mathrm{N}+1$. Then, the four subsets of the filter window W can be expressed [23] as:

$$\begin{cases} W_1(i,j) = \{X(i, j+k);\ -N \le k \le N\} \\ W_2(i,j) = \{X(i+k, j+k);\ -N \le k \le N\} \\ W_3(i,j) = \{X(i+k, j);\ -N \le k \le N\} \\ W_4(i,j) = \{X(i+k, j-k);\ -N \le k \le N\}, \end{cases} \tag{1}$$

Obviously, they represent a one-dimensional window that is 45°, 135°, horizontally, vertically, and horizontally. Let $Z_1(m, n)$, $Z_2(m, n)$, $Z_3(m, n)$, and $Z_4(m, n)$ be the median gray values of the pixels in the four sub-windows, that is,

$$\begin{cases} Z_1(i,j) = med[x(i,j) \in W_1(m,n)] \\ Z_2(i,j) = med[x(i,j) \in W_2(m,n)] \\ Z_3(i,j) = med[x(i,j) \in W_3(m,n)] \\ Z_4(i,j) = med[x(i,j) \in W_4(m,n)], \end{cases} \tag{2}$$

The output of the multilevel median filter is defined [23] as:

$$Y(i,j) = med[Y_{\min}(i,j), Y_{\max}(i,j), X(i,j)], \tag{3}$$

The output of the weighted multistage median filter is:

$$Y(i,j) = \sum_{s=1}^{4} Z_s(i,j)/4, \tag{4}$$

The gray value median values of the four sub-windows are then averaged to be the gray value of the pixel to be sought. The effect of median filter filtering depends on the size and shape of the filter window. If the window size is chosen too large, although there is strong denoising ability, the details and edges of the image are seriously lost, which makes the image blurred; if the size is chosen too small, although the details can be preserved, the noise reduction effect will be worse. But this problem can be solved by adding a two-dimensional filter mask.

2) TWO-DIMENSIONAL FILTER MASK COMBINED WITH WEIGHTED MULTISTAGE MEDIAN FILTER

Based on the weighted multistage median filter, three three-dimensional filter mask windows with different sizes are added to the four one-dimensional filter windows to filter the image by selecting windows of different sizes and shapes in different image regions. Since the mask size and the shape of different image regions are different, the possibility of erroneously culling edge information can be reduced, and more detailed features are retained while removing noise. These 7 windows can be explained [24] as:

$$\begin{cases} W_1(i,j) = \{X(i-m, j-n);\ -1 \le m \le 1, -1 \le n \le 1\} \\ W_2(i,j) = \{X(i-m, j-n);\ -2 \le m \le 2, -2 \le n \le 2\} \\ W_3(i,j) = \{X(i-m, j-n);\ -3 \le m \le 3, -3 \le n \le 3\} \\ W_4(i,j) = \{X(i, j-m);\ -3 \le m \le 3\} \\ W_5(i,j) = \{X(i-m, j);\ -3 \le m \le 3\} \\ W_6(i,j) = \{X(i+m, j-m);\ -3 \le m \le 3\} \\ W_7(i,j) = \{X(i-m, j-m);\ -3 \le m \le 3\}, \end{cases} \tag{5}$$

The relationship is shown in Table 2. W_1 is the two-dimensional mask filtering window of 3×3; W_2 is the two-dimensional mask filtering window of 5×5; W_3 is the two-dimensional mask filtering window of 7×7; $W_4 - W_7$ is the same as the formula (1).

The basic process after improvement is as follows. Firstly, the initial pixel position in the rice disease image is determined, and then the variance of the gray value of each window is calculated centered on the point; then, the two-dimensional window is compared; when the variance of the two-dimensional window is smaller than the threshold, the window with the smallest variance is selected as the filtering window. Otherwise, the one-dimensional window with the smallest variance is chosen to be the filtering window; finally, the filtering window is subjected to the median filtering process. This will better preserve the details of the rice leaf picture.

TABLE 2. Meaning of variables.

Variable	Meaning
W_1	2D mask filtering window of 3×3
W_2	2D mask filtering window of 5×5
W_3	2D mask filtering window of 7×7
W_4	1D filtering window along the horizontal direction
W_5	1D filtering window along the vertical direction
W_6	1D filtering window with $45°$ horizontal direction
W_7	1D filtering window with $135°$ horizontal direction

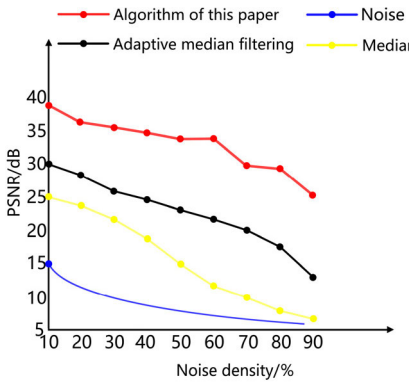

FIGURE 4. The image noise rate after processing by different algorithms.

The results of the noise reduction treatment of rice disease images using the algorithm, the adaptive median filtering algorithm and median filtering are shown in Fig. 4. Under different noise densities, the noise reduction performance of this algorithm is higher than that of other algorithms. With increasing noise density, the performance of median filtering and the adaptive median filtering algorithm decreases rapidly. However, the algorithm in this paper is stable. When the noise density is 90%, it still maintains a good denoising effect.

C. IMAGE SEGMENTATION PROCESSING BASED ON FASTER 2D-OTSU

In the picture of rice diseases after the noise reduction treatment, there are other backgrounds besides the target rice leaves, which will cause interference and reduce detection accuracy. In order to facilitate the detection and expansion of data sets, we need to separate the target rice leaves from the background, that is, image segmentation processing. Threshold segmentation is more common and simple to operate. Therefore, this paper uses the threshold segmentation method to segment the image.

Otsu' algorithm proposed by the Japanese scholar Otsu in 1978 is called the maximum inter-class variance method, and is one of the mainstream algorithms of the threshold segmentation method with excellent segmentation effect. However, the traditional one-dimensional Otsu method only considers the gray information of the image, but fails to fully take the spatial information of the image into account [25]–[27]. Therefore, when the image histogram does not show obvious double peaks, the information loss

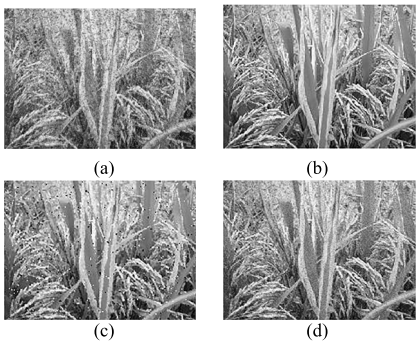

FIGURE 5. Image preprocessing effect: (a) Original image. (b) Algorithm of this paper. (c) Adaptive median filter. (d) Median filter.

will occur when the method is used for segmentation. In the conventional two-dimensional (2D) Otsu algorithm, as the two-dimensional histogram composed of the gray value of the image neighborhood and its neighborhood mean is mainly used to segment, it shows excellent anti-noise performance, but its complexity is high. Therefore, in this text, a Faster 2D-Otsu algorithm is employed to decompose the conventional 2D Otsu algorithm into two one-dimensional Otsu algorithms, that is, the original rice disease image $f(x, y)$ obtains a threshold s, its neighborhood mean image. $G(x, y)$ gets a threshold t. From the perspective of the computer, solving the two thresholds for replacing the threshold of the original 2D Otsu algorithm not only lowers the time complexity of the algorithm, but also reduces the storage space of the computer. In addition, considering the strong correlation between the rice disease target class and the background class internal pixels, this text comprehensively studies the concept of inter-class variance and intra-class variance, and introduces a new threshold discriminant function.

Let the threshold s divide a set of discrete data into two categories, and the variance between the classes is:

$$s_p = w_0 w_1 (u_0 - u_1)^2, \tag{6}$$

where u_0 and u_1 represent the mean of the target class and the background class, respectively; w_0 and w_1 refer to the probability of the target and the background class, accordingly. Therefore, the larger the s_p value, that is, the larger the variance between classes, the more obvious the distinction between the target class and the background class, and the better the segmentation effect.

Let the threshold s divide a group of discrete data into two categories. p_i denotes the probability of occurrence of i, u_0 and u_1 respectively represent the mean of the two types, and w_0, w_1 refer to the probability of two types separately. Then, the variances of the two types of data in the class are respectively indicated as:

$$s_1 = \sum_{i=0}^{s} p_i (i - u_0)^2, \tag{7}$$

$$s_2 = \sum_{i=S+1}^{L-1} p_i (i - u_1)^2, \tag{8}$$

Then the total variance within the two classes is:

$$s_w = w_0 s_1 + w_1 s_2 \tag{9}$$

Obviously, s_w represents the cohesiveness of the two types of data in this group of data. The smaller the value, the better the segmentation effect. As for the two factors of inter-class variance and intra-class variance, the larger the variance between classes, the smaller the intra-class variance and the better the segmentation effect obtained. There is a necessity to introduce a new discriminant function, that is, the intra-class class variance ratio method:

$$\mathrm{S} = s_p / s_w, \tag{10}$$

Then the optimal threshold satisfies $S* = \arg\max\{S\}$, and the corresponding gray value is the optimal threshold. Similar to the optimal threshold t of the neighborhood mean image g(x, y), the method avoids exhaustive traversal in the L×L dimension, and only needs to find the optimal threshold in two spaces of length L, which reduces the amount of calculations and the storage space required by the computer. The algorithm steps are as follows:

Step 1: Initial threshold range calculation

Since the target gray level of the rice disease image is inevitably higher than the mean of a large number of backgrounds, the lower limit of the initial threshold is set to the image gray mean m, and the experiment confirms the conclusion. In addition, since the target gray level of the rice disease image is inevitably not higher than the maximum gray value of the image, the upper limit of the initial threshold is set as the maximum gray value n of the image.

Step 2: The optimal threshold

In order to further reduce the computation time, in this paper, the two-dimensional image gray matrix is converted into a one-dimensional matrix (1, L), and the variance between the image classes s_p and the intra-class variance s_w are obtained according to equations (6) and (9). Then, the optimal threshold s is acquired according to equation (6), and the optimal threshold t of the neighborhood mean image $g(x, y)$ can also be obtained.

Step 3: Split images

The rice disease image segmented by the Faster 2D-Otsu is shown in Fig. 6. As can be seen from the figure, most of the lesions have been extracted.

D. RAPID DETECTION OF RICE DISEASE BASED ON FCM-KM AND FASTER R-CNN FUSION

In the picture after the elapse of segmentation, the location and features of rice diseases are prominent, which satisfies the conditions for image detection. Convolutional neural networks have developed rapidly in terms of image detection and achieved good results. Convolutional neural networks are applied to target detection in two stages: The Two stage and the One stage. Compared with the Two stage method, the One stage method does not need to extract the candidate region of the target, and the speed is faster. Nevertheless, the detection precision is not as good as that of the Two stage method.

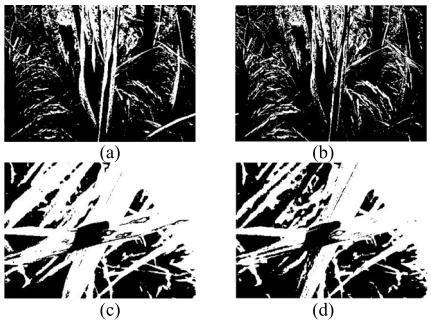

FIGURE 6. Threshold segmentation: (a), (c) Faster 2D-Otsu. (b), (d) Otsu threshold segmentation.

The Faster R-CNN in the Two stage method can basically realize real-time detection under GPU acceleration [28]. However, the traditional fast R-CNN algorithm generates a large number of bounding boxes, and the detection speed and accuracy are still not ideal. To solve this problem, we have proposed a method for detecting rapid rice disease based on FCM-KM and fast R-CNN fusion.

The K-Means clustering algorithm exhibits the advantages of fast convergence and simple calculation process. However, there is no definite algorithm for selecting the K value. An unreasonable selection of the K value would have a severe impact on the precision and computational complexity of clustering. Moreover, the optimal result of clustering corresponds to the extreme point of the objective function, which the clustering center falls near a certain local minimum point, which tends to cause makes the algorithm prone to falling into local optimum. In view of the drawbacks as mentioned above, an FCM-KM algorithm is proposed. Firstly, the algorithm relies on the maximum and minimum distance algorithm to determine the size of the cluster center K and where the initial cluster center is positioned. Then, the Tent chaotic map with uniform ergodicity and fast iteration is applied to the construction of the chaotic search space with the initial cluster center as the reference point. The initial clustering center is optimized by conducting Tent chaotic search, which causes the algorithm to jump out of local optimum and obtain faster convergence speed. Finally, the location update formula of intelligent firefly optimization algorithm is applied to categorize the clustering of non-clustered center sample points, thus completing the clustering process.

1) INTRODUCTION TO FASTER R-CNN

The team of the target detection community, Ross Girshick, launched a new effort Faster R-CNN [21] in 2015, which was after the launch of R-CNN [29] and Fast R-CNN [30]. Faster R-CNN does not have a fixed size requirement for the image of rice diseases to be detected. As an input image, it merely needs to be scaled to a certain extent in length and width, so distortion can be avoided. After the improvement of RPN, the detection speed is greatly improved. Faster R-CNN can be simply viewed as a model of ''the regional generation network + Fast R-CNN'', which applies the Region Proposal

Network (RPN) instead of Selective Search in Fast R-CNN. RPN is a recommendation algorithm for the proposal. The convolution layer/full connection layer processing is performed on the feature map, and then the detected target is subjected to position regression and the classification, and finally the region recommendation is used to obtain a more accurate disease location. Fast R-CNN is in line with the detailed calculation of the position of the frame and the category of the objects in the frame.

(a) Faster R-CNN steps:

Step 1: Input the entire picture of rice diseases into CNN to obtain a feature map;

Step 2: The convolution feature is input to the RPN to acquire the feature information of the candidate frame;

Step 3: Identify the characteristics of rice diseases extracted from the candidate box, and use a classifier to determine whether it belongs to a specific disease category;

Step 4: For the candidate frame belonging to a certain disease feature, the position of the disease is further adjusted by a regression device.

(b) Generate RPNs for candidate regions

The regional generation network is referred to as RPN, and its core idea is to directly generate suggested areas using the CNN convolutional neural network. After inputting the picture of rice diseases into the shared convolution network, we observe that the feature map is obtained as the input of the RPN network, and the points of the convolutional feature map are corresponding to the position of the original pictures [31]. The elements on each feature map correspond to 9 anchor boxes with different sizes. The RPN itself has two convolutional networks, one of which has an 18-dimensional convolution operation through a 1×1 convolution kernel to determine whether the anchor box is a foreground image; the other convolution structure passes a 1×1 volume. The accumulative kernel performs a 36-dimensional convolution operation to obtain the relative position coordinates of the bounding box for Ground Truth, and obtain the relative position coordinates $dx(A)$, $dy(A)$ and $dw(A)$ of the bounding box for Ground Truth. The setting method of the nine bounding boxes corresponding to each feature map element is: The point of the convolved feature map is mapped to the position of the original picture, and each point on the feature map is mapped onto the original picture (each pixel is set as an ''anchor point'') [32]. In this way, several anchors of different sizes (that is, the surrounding bounding boxes) are placed on each anchor point. The commonly used scales are 128^2, 256^2, and 512^2, and three different aspect ratios of 1:1, 1:2, and 2:1, respectively.

In the Proposal layer of the RPN, the new rectangular position obtained by the anchor is first adjusted according to the adjustment parameters. To avoid the new area being too small, enter im_info, the classification result after the classifier, and the relative position coordinates after returning to the anchor box, and use these values to pass non-maximum suppression and other filtering means, and then get the regression. For the candidate regions of the original image, the coordinates of the lower left corner and the upper corner of each candidate region output candidate region are output.

RPN steps: (1) slide a window on a rice diseases map; (2) establish a neural network for the classification of rice diseases and the return of the frame position; (3) the position of the sliding window offers general location information of rice diseases; (4) the regression of the box provides a more accurate location of rice diseases.

(c) Feature extraction

The image processed by the RPN is sent to the RoI Pooling layer to pool the rice disease areas. The Faster R-CNN algorithm proposes a region of interest (RoI Pooling) by further improving the SPP-Net algorithm. The RoI Pooling layer is used to convert a range of dimensions to a fixed size to meet the requirements of the next fully connected network layer. The ROI Pooling layer evenly divides each rice disease candidate area into $M\times N$ blocks, and performs max pooling on each block [33]. The disease candidate areas of different sizes on the rice diseases map are transformed into uniform data and sent to the next layer. Although the size of the input image and the feature map is different, we can extract a feature representation of a fixed dimension for each region by adding the ROI Pooling layer, so that the diseases can be classified later.

(d) Classification regression and location refinement

Considering the pictures of rice diseases that have been identified, we classify diseases and refine the location. The classification steps are: firstly, object or non-object classification for each of two regions corresponding Anchor Box, k then regression models (each corresponding to a different Anchor Box) Rice Diseases trimming candidate frame location and size, and in the end, the target is classified. The formula for calculating the fully-connected layer of the classification is as follows:

$$(x_1, x_2, x_3)\begin{pmatrix} w_{11}w_{12} \\ w_{21}w_{22} \\ w_{31}w_{32} \end{pmatrix} + (b_1, b_2) = (y_1, y_2), \qquad (11)$$

The position detection of rice diseases is measured by the size of the overlap area. Some of the seemingly accurate test results are often due to the inaccuracy of the candidate frame and the small overlap area. Therefore, a step of intensive repair of rice diseases is needed. The eigenvectors obtained in the classification section are calculated and classified by full connection and Softmax, and the probability of a species pertaining to a certain rice diseases species is output. Through the anchor box regression, the offset of this region from the real GT position is obtained for subsequent regression, which makes the rice diseases detection frame closer to the real position.

(e) The training processes

This experiment was carried out on the Caffe deep learning framework, and the training set of the rice diseases and the disease was randomly sent to the neural network for training. After training the model, we test it to get the test results and

analyze them. The steps of the Faster R-CNN training model are as follows:

Step 1: Train the RPN after initializing the RPN network with the model (the pre-training model). After the training is completed, the unique value of the model and the RPN will be updated;

Step 2: Initialize the Faster R-CNN network with the model, and then use the trained RPN to calculate the proposal. Next, we give the proposal to the Faster R-CNN network, and then train the Faster R-CNN. After the training, the model and the unique of the Faster R-CNN will be updated.

Step 3: Initialize the RPN network using the model completed in the second step and perform a second training on the RPN network. During the training process, the model parameters are always unaltered, but the unique value of the RPN is changed.

Step 4: Keep the model parameters unchanged in the third step; initialize the Faster R-CNN; train the Faster R-CNN network for the second time to fine-tune the parameters.

2) THE K-MEANS CLUSTERING ALGORITHM

The K-Means clustering algorithm is a typical unsupervised learning algorithm, which is mainly used to classify samples (n) into k categories [34]. First input n samples, set the number of categories k to be separated, and randomly extract k points from n samples as the center point of the first cluster; then, calculate the distance from n samples to k cluster centers, and classify the n samples for calculating the average of all samples of each class to get a new cluster center. Set a criterion function and repeat the above steps until the result is consistent with this criterion function, and the final clustering result is obtained. The K-means algorithm determines the similarity of samples based on Euclidean distance; the formula is:

$$d(X_i, X_j) = \sqrt{\sum_{k=1}^{m} (X_{ik} - X_{jk})^2}, \tag{12}$$

From the above process, it can be seen that the K-Means displays the advantages of simplicity and easy understandability. It is also characterized by fast convergence speed and low time complexity, in addition to being effective in processing large-scale data sets and insensitive to the input order [35]. For the traditional K-means algorithm, after the initial cluster center is given, the randomness and global search ability of the firefly algorithm can be used for more precise classification of the data sets except the cluster center, thereby further improving the convergence speed of the algorithm and achieving the optimization of the K-means algorithm. However, the firefly-optimized K-means algorithm remains subjected to the following drawbacks:

(1) There is no definite algorithm for selecting the value K of the cluster center. An unreasonable selection of K value would have a severe impact on the accuracy and computational complexity of clustering.

(2) The result of optimal clustering corresponds to the extreme point of the objective function, and the clustering center falls near a certain local minimum point, which makes the algorithm easy to fall into local optimum.

Based on the mutual attraction of fireflies, the K-means clustering process is used to improve the convergence speed of global search. In view of the drawbacks to the existing algorithms in global optimization search, it is easy to fall into local extremum regions. With the characteristics of sensitivity and ergodicity, a dynamic population firefly algorithm (FCM algorithm) based on the chaos theory as well as the maximum and minimum distance algorithm is adopted to improve K-means clustering [36]–[41].

3) OPTIMIZATION OF K-MEANS CLUSTERING ALGORITHM

(a) Firefly algorithm

The algorithm simulates the movement process of the firefly, and then assigns its objective function value and calculates the relative attractiveness according to the position and fluorescence brightness of each firefly. Individuals with stronger fluorescence attract individuals with weaker fluorescence to move according to the position update formula, and the moving distance is determined by the size of the attraction. The optimization process is based on the following three principles:

(1) The gender factor of fireflies is ignored, and any two firefly individuals can attract each other.

(2) The attraction of fireflies is inversely proportional to the distance and proportional to the brightness. Fireflies with strong brightness attract the fireflies with weak brightness to move, and the individuals with the strongest brightness move randomly;

(3) The brightness of a firefly individual is determined by the value of the objective function at its location.

Fluorescence brightness is:

$$I \propto -f(x_i), 1 \le i \le n, \tag{13}$$

$$I = I_0 \exp(-\gamma * r_{ij}), \tag{14}$$

where I represents the fluorescence brightness, and $f(x_i)$ represents the objective function, x_i is the spatial position of the firefly i; I_0 represents the maximum fluorescence brightness; γ is a constant indicating the light absorption coefficient; r_{ij} is the Euclidean distance between x_i and x_j.

The attraction is

$$\beta = \beta_0 \exp(-\gamma * r_{ij}^2), \tag{15}$$

Among them, β_0 is the maximum attractiveness.

The location update formula is

$$\beta = \beta_0 \exp(-\gamma * r_{ij}^2), \tag{16}$$

where α represents the step factor of the initialization; ε_i represents the random factor obeying the Gaussian distribution.

(b) The maximum and minimum distance algorithm determines the cluster center value K

The Max-Min distance clustering algorithm is similar to the traditional K-means. They calculate the Euclidean distance and classify the sample points belonging to each cluster center according to the nearest neighbor principle. The difference is that the former does not directly give the cluster category value K, instead, one object X_i is selected from the sample points as the first cluster center, and then the Euclidean distance from each point to X_i is calculated by the formula (12), and the point farthest from the distance X_i is taken as the new cluster center. The above division steps are repeated until a new cluster center is no longer generated, and finally the total number K of cluster centers is determined. The algorithm steps are as follows:

Step1: Given A and B, and select the initial cluster center;

Step2: Generate a new cluster center:

By calculating the Euclidean distance D_{i1} from each point to Z_1, the x_k corresponding to $D_{k1} = \max\{D_{i1}\}$ is selected as the next cluster center Z_2;

Calculate the distance D_{i1}, D_{i2} from each point to cluster centers Z_1 and Z_2. If $D_i = \max\{\min(D_{i1}, D_{i2})\}$, $i = 1, 2, \cdots, n$, and $D_i > \theta * D_{12}$, then x_i is taken as the third cluster center Z_3.

$$\begin{cases} D_{i1} = \|x_i - Z_1\| = \sqrt{\sum_{i=1}^{d} |x_i - Z_1|^2} \\ D_{i2} = \|x_i - Z_2\|, \end{cases} \tag{17}$$

If Z_3 exists, it is judged whether there is $D_j = \max\{\min(D_{i1}, D_{i2}, D_{i3})\}$. If the above conditions are met and $D_i > \theta * D_{12}$ determines the fourth cluster center. And so on, if $D_i \leq \theta * D_{12}$ appears, stop looking for a new cluster center.

Step3: Statistics total number of cluster centers K

The clustering result of the algorithm is related to the selection of parameters and starting points. In order to obtain a good clustering effect, it is necessary to carry out repeated experiments without prior knowledge of sample distribution. Therefore, this algorithm is only used to determine the value of the clustering center value K in this paper.

(c) Chaos Theory Optimization Cluster Center

In order to avoid the clustering center of the firefly-optimized K-means algorithm falling near a certain local minimum point and improve the global search ability of the algorithm, and then jump out of the local optimal solution, this paper uses the chaotic theory cluster K-means. The optimization process is performed because chaotic variables are random, ergodic and regular. Since the Logistic chaotic map is concentrated in the 0, 1 boundary range, there is a significant ergodic unevenness problem, which leads to low algorithm efficiency. Many scholars proved through rigorous reasoning that the chaotic sequence generated by Tent map is more helpful to algorithm optimization, and points out that the convergence speed and ergodic uniformity of Tent map are better than logistic mapping [42].

• Tent chaotic sequence

The Tent mapping expression is:

$$x_{t+1} = \begin{cases} 2x_t, 0 \leq x_t \leq \frac{1}{2} \\ 2(1 - x_t), \frac{1}{2} \leq x_t \leq 1, \end{cases} \tag{18}$$

The Tent map is transformed by Bernoulli shift and is expressed as:

$$x_{t+1} = (2x_t) \bmod 1, \tag{19}$$

The steps for generating a Tent chaotic sequence are as follows:

Step1: Randomly generate an initial value x_0 that is not in the range of (0.20,0.40,0.60,0.80), denoted as z, $z(1) = x_0$, $i = j = 1$

Step 2: Iterate according to equation (7) to generate sequence x.

Step3: If $x(i) = [0, 0.25, 0.5, 0.75]$ or $x(i) = x(i - k)$, $k = [0, 1, 2, 3, 4]$, perform step 2

Step4: Change the initial value of iteration according to formula $x(i) = z(j + 1)$, $j = j + 1$, and perform step 2

Step5: If the maximum number of iterations is reached, the operation is terminated and the generated x sequence is saved.

• Chaotic search

The FCM algorithm adopted in this paper generates a Tent chaotic sequence based on the locally searched local optimal solution, and jumps out the local optimum through Tent search to obtain the global optimal solution. The specific plan is as follows:

The distance D_{ix} between each cluster center $C_i (i = 1, 2, \cdots, k)$ and the current cluster center C_x is arranged in order from large to small, and the first n (accounting for 30% of the total number of cluster centers) $C_{i1}, C_{i2}, \cdots, C_{in}$ and C_x are obtained. And find the maximum value $X^j_{\max}$ and the minimum value $X^j_{\min}$ of the j-th dimension in the current $n+1$ class to form a new chaotic search space.

Suppose the cluster center is $C_x, X_k = \{x_{k1}, x_{k2}, \cdots, x_{kd}\}$, then the main steps of Tent chaos search are:

Step 1: Use $z^0_{kj} = (x_{kj} - X^j_{\min})/(X^j_{\max} - X^j_{\min})$ to map X_x to (0,1), where $k = 1, 2, \cdots, n, j = 1, 2, \cdots, D$.

Step 2: Substituting the above formula into equation (19) for Tent mapping, iteratively generates chaotic variable sequence $z^m_{kj} (m = 1, 2, \cdots, C_{\max})$, where $C_{\max}$ is the maximum number of iterations of chaotic search.

Step 3: Use equation (20) to restore z^m_{kj} to the neighborhood of the original solution space, and generate a new solution v_k.

$$v_{kj} = x_{kj} + (X^j_{\max} - X^j_{\min}) * (2z^m_{kj} - 1)/2, \tag{20}$$

Step 4: Calculate the fluorescence brightness value $F(v_k)$ of v_k and compare it with the fluorescence brightness value $F(x_k)$ of the local optimal solution to retain the best solution.

Step 5: If the number of searches reaches $C_{\max}$, stop searching; otherwise, go to step 2.

(d) Fusion of FCM-KM algorithm and Faster R-CNN algorithm

• Basic steps of the FCM-KM algorithm

Step 1: Initialization parameters: total number of clustering objects N, absorption coefficient γ, step factor α, maximum number of iterations of chaotic search $C_{\max}$, maximum fluorescence brightness I, maximum attraction β_0.

Step 2: Determine the number of cluster centers K by the maximum and minimum distance algorithm, and record the initial cluster center position obtained by the maximum and minimum distance algorithm.

Step 3: Construct a chaotic search space with each cluster center as a reference point through Tent mapping.

Step 4: Use the Tent chaotic search to update the position of the initial cluster center until the cluster center no longer changes.

Step 5: The cluster center corresponds to the target firefly, giving the highest fluorescence brightness. Calculate the Euclidean distance of the remaining sample points relative to each cluster center and assign different fluorescence brightness according to formula (14).

Step 6: If $I_i > I_j$, it means that Firefly j is smaller than i's objective function value, that is, j is better than i, then Firefly j will attract i to move to it. The movement mode is determined by the formula (15), and the firefly position is updated by the equation (16).

Step 7: Repeat step 6 until all fireflies are divided into their own cluster centers.

• Fusion of FCM-KM algorithm and Faster R-CNN algorithm

The Faster R-CNN algorithm uses the RPN innovatively, the area suggestion network generates 9 area frames of different sizes in the respective positions of the last feature layer, where the size and the ratio of the area frame are preset, and Do not change according to the size of the target in the dataset., the speed of training and detection will be relatively slow. The FCM-KM algorithm solves the problem that the initialization parameter setting of the traditional K-means clustering algorithm is easy to fall into the local optimum and improves the convergence speed. Based on this, this paper improves the Faster R-CNN algorithm by FCM-KM algorithm and resets the size of the bounding box. The specific steps of the FCM-KM algorithm and the Faster R-CNN algorithm are shown in Figure 8. The brief steps are as follows:

Step 1: Labeling of three rice disease training sets, the image annotation tool VIA is utilized to perform this work, Figure 7 is part of the mark data set involved in this paper. The original image contains the color, shape, and texture characteristics of the disease. Despite this, some of the marker boxes still contain a large proportion of other areas. In order to prevent the influence exerted by other areas and make the network capable of fully extracting the characteristics of the disease, the data set image involved in this paper contains both the original color image and the segmented image, as shown in Figure 7.

Step 2: Reading the left and upper right corners of all targets (no disease types) in the training set file, and get the size of the target frame by doing the difference, as the input of the FCM K-Means clustering algorithm. Then cluster analysis of the target frame size in the rice disease data set.

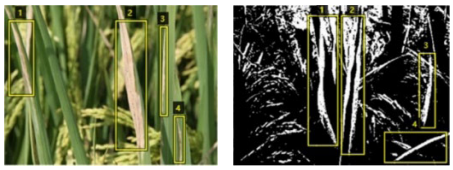

FIGURE 7. Original color image and segmented image.

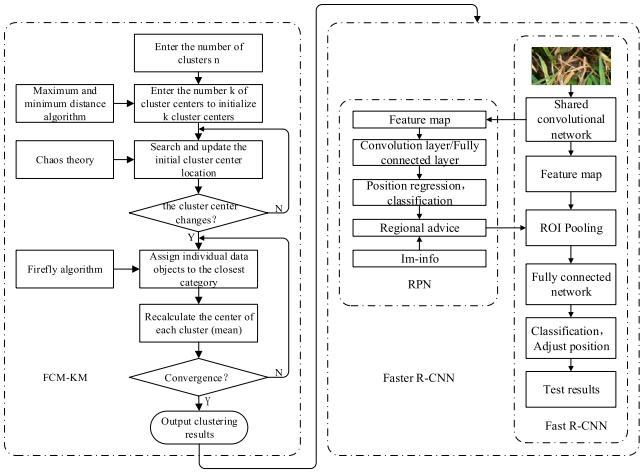

FIGURE 8. Rapid detection of rice disease based on FCM-KM and Faster R-CNN fusion.

Step 3: The cluster center is taken as input for the traditional Faster R-CNN framework, and the new bounding box scale is set to perform the training of the Faster R-CNN network. The specific approach to input of the Faster R-CNN by the cluster center is as follows. The return value of the FCM-KM algorithm, that is, the cluster category value K and its cluster center, are passed to the generate_anchors function in the initial candidate box generation file generate_anchor.py, with clustering The center as the replacement of the aspect ratio value (0.5, 1, 2) of the original candidate frame.

Finally, the number of clustering categories k = 4 is obtained by applying the maximum and minimum distance algorithm, for which it is necessary to increase the proportion of the bounding box on the basis of the original. Nevertheless, the rising number of bounding box is adverse to improving the convergence speed. Despite this, the standard Faster R-CNN network model is designed specifically for the 20-category task of the standard data set VOC2007. The rice disease portion occupies only a tiny proportion of the entire image when compared to the size of the target category such as airplane, car, and horse in the standard VOC2007 data set, for which it is classed as a small goal. Therefore, the size of $512^2$is excessively redundant for rice diseases, thus resulting in an excessive amount of initial frame shifting during positional refinement, which makes it likely to cause frame inaccuracy.

TABLE 3. Average clustering accuracy of the algorithm.

Data	K-Means	FCM-KM
Rice blast	87.96%	92.16%
Bacterial blight	80.51%	90.75%
Sheath blight	79.97%	88.72%

Therefore, the candidate frame of this size is abandoned in this paper so as to improve the accuracy of detection. The new proportion of the clustering center, i.e., the bounding box, ends up being 1.46, 1.81, 1.24, 1.42, respectively.

In view of the fact that the parameter setting of the firefly algorithm has a great influence on the experimental results, this paper uses the horizontal experiment to obtain the combination with the most frequent occurrences of the optimal solution. That is, the step size factor α and the light intensity absorption coefficient γ are enumerated to obtain a series of optimal value combinations. The final parameter is set to: The maximum attractiveness $\beta_0 = 100$, the absorption coefficient $\gamma = 1$, the step factor $\alpha = 0.06$, the maximum number of iterations $C_{\max} = 50$, the maximum fluorescence brightness $I = 100$, $\theta = 0.4$.

From Figure 9, we can see that the distribution of some cluster centers in the traditional K-means algorithm is more concentrated, and there are obvious local optimal problems. Compared with the K-means algorithm, the FCM-KM algorithm proposed in this paper has a more uniform cluster center distribution, which significantly improves the problem of easy to fall into local optimum, and the clustering effect is better. In addition, the convergence curves of the FCM-KM algorithm and the K-Means algorithm on the three data sets are shown in Fig. 10. Obviously, on these three data sets, the overall convergence speed and convergence degree of the FCM-KM algorithm are due to the traditional K-Means algorithm. It can be seen from Table 3 that the algorithm firstly determines the cluster center value K by the maximum and minimum distance algorithm and introduces the chaos theory to optimize the cluster center. The average clustering accuracy is 7.73% higher than the classical K-means algorithm.

IV. APPLICATION AND RESULTS ANALYSIS

In order to verify the effectiveness of the algorithm and the efficiency of parallel optimization, the simulation environment of this experiment is windows 10 operating system, CPU processor is i7 four generation processor, solid state hard disk 250G, memory is 16GB, CPU processor is NVIDIA 1080 Ti. The experimental platform is Ubuntu 14.04, and the Caffe framework is chosen as the deep learning framework. The data set used incorporates three categories (the rice blast, bacterial blight, and sheath blight) for a total of 3,010 images, 60% of which were used for training sets, 20% for verification sets, and 20% for test sets. The final number of iterations is set to 15000 and the learning rate is 0.001.

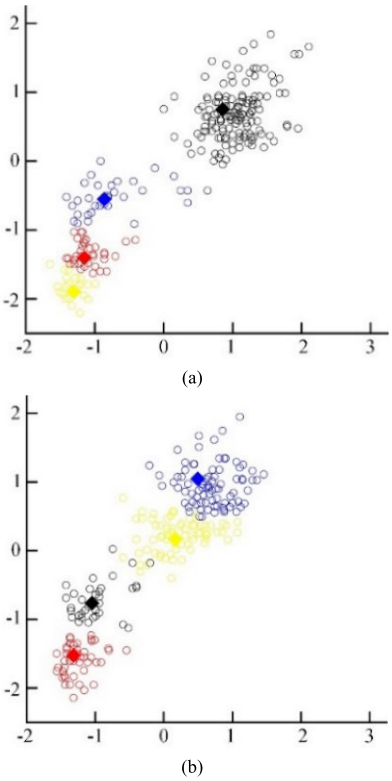

FIGURE 9. (a) K-Means algorithm clustering effect. (b) FCM-KM algorithm clustering effect.

A. TEST RESULTS

1) RICE BLAST

For the rice blast, the recognition results are shown in Figure 11, which indicates that the method put forward in this paper can accurately identify rice blast lesions. It can be found from Figure 12. a, the accuracy rate of Faster R-CNN reaches 50.00% when trained to about 800 rounds, and the recognition accuracy of rice diseases reaches 90.00% after trained 1300 times. Then, from Figure 12. b, the recognition accuracy of the improved Faster R-CNN is completed in training. At last, it reaches 96.71%, and the recognition accuracy reaches 50% when trained to around 600 rounds. After that, it can be clearly seen from Fig. 13 that the loss function of the algorithm at the beginning of the training is lower than that of the unmodified Faster R-CNN algorithm, and can converge to a stable state more quickly. This is because the bounding box size in this paper is set corresponding to the data set in this paper, so during the training, the steps such as bounding box regression can quickly adjust the candidate area to a position close to the detection target frame. Figure 14 shows the roc curves for the two algorithms of the rice blast data set. We can see that the Faster R-CNN curve after fusion with FCM-KM is closest to the upper left corner, indicating that its True Positive Rate (TPR) is higher when its False Positive Rate (FPR) is lower, which means that the detection method is more effective. Besides, it can be observed from Table 4 that the training time is 103.4 min when the Faster R-CNN iterates 10000 times; the training

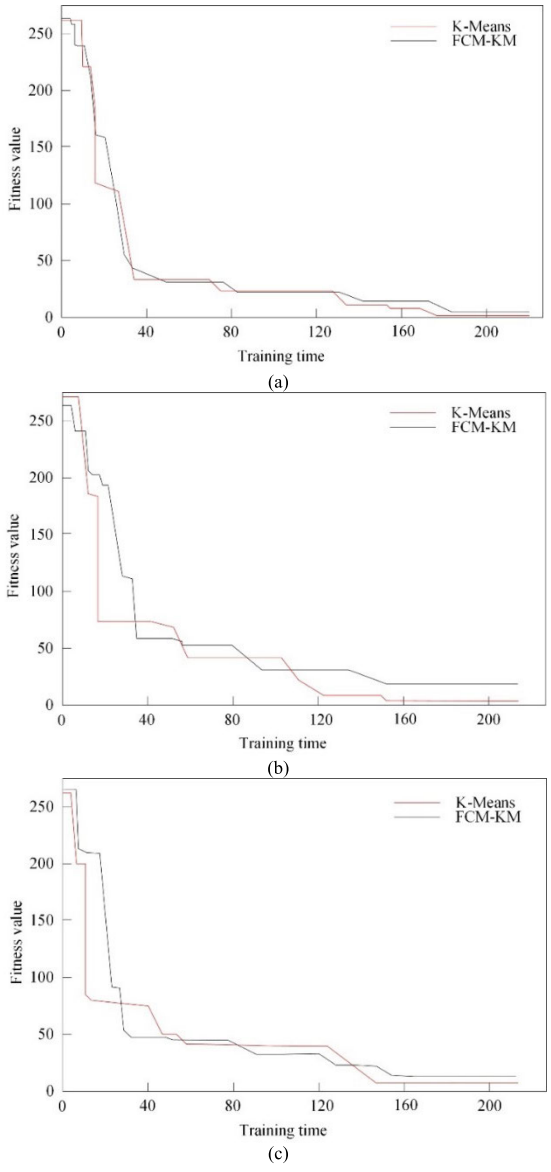

FIGURE 10. (a) Convergence curves of two algorithms on rice blast dataset. (b) Convergence curves of two algorithms on the bacterial leaf blight dataset. (c) Convergence curves of two algorithms on the sheath blight dataset.

TABLE 4. Comparison of different network iterations and training time in rice blast.

Faster R-CNN		FCM-KM + Faster R-CNN	
Number of iterations	Training time/min	Number of iterations	Training time/min
10000	103.4	8000	69.1

time is 69.1 min when the improved Faster R-CNN iterates 8000 times.

2) BACTERIAL LEAF BLIGHT

For bacterial leaf blight, the recognition results are shown in Figure 15, signifying that the method proposed can precisely identify the bacterial leaf spot. As can be seen from

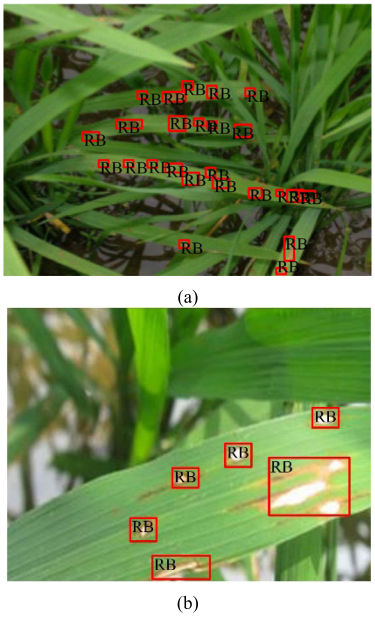

FIGURE 11. Rice blast recognition effect.

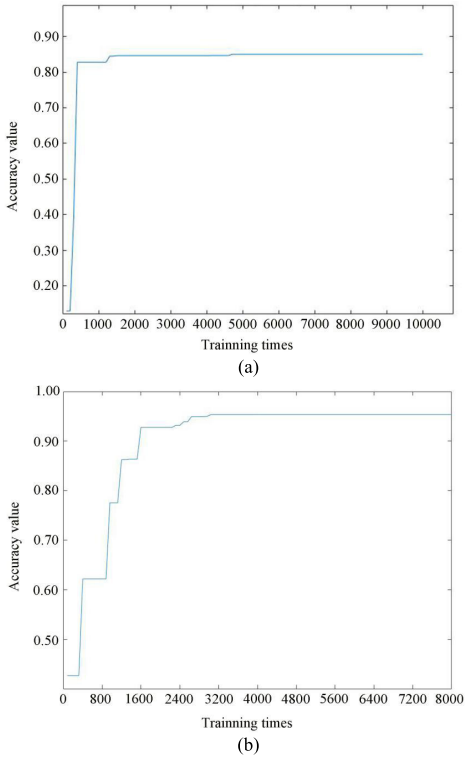

FIGURE 12. The recognition rate of the rice blast: (a) Faster R-CNN recognition rate. (b) FCM-KM + faster R-CNN recognition rate.

Figure 16. a, the accuracy rate of Faster R-CNN reached 50.00% when trained to about 750 rounds, and the recognition accuracy of rice diseases reached 90.00% after trained 2000 times. From Figure 16. b, the recognition accuracy of the improved Faster R-CNN is completed in training. After that, it reached 97.53, and the recognition accuracy reached 50% when trained to about 300 rounds. Next, from

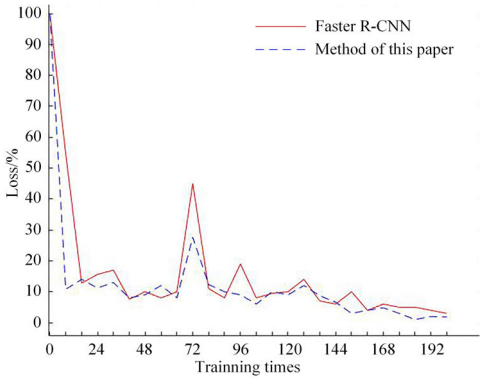

FIGURE 13. Loss function line chart for rice blast.

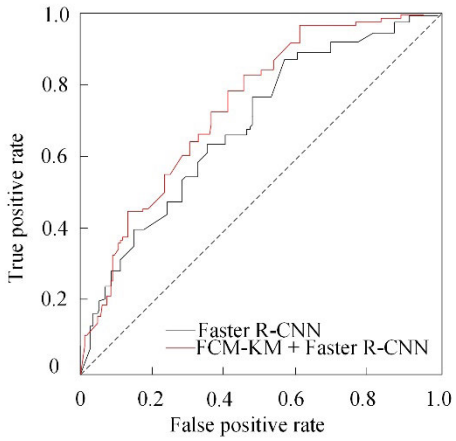

FIGURE 14. ROC curve of two algorithms about rice blast.

TABLE 5. Comparison of different network iterations and training time in bacterial leaf blight.

Faster R-CNN		FCM-KM + Faster R-CNN	
Number of iterations	Training time/min	Number of iterations	Training time/min
10000	111.2	8000	78.7

Fig. 17, we can see that the loss function of the algorithm in the training process is lower than that of the unmodified Faster R-CNN algorithm, and can converge to a stable state more quickly. Figure 18 shows the roc curves for the two algorithms of the rice blast data set. We can see that the Faster R-CNN curve after fusion with FCM-KM is closest to the upper left corner, indicating that its TPR is higher when its FPR is lower, which means that the detection method is more effective. In addition, Table 5 shows that when the Faster R-CNN iteration is 10,000 times, the training time is 111.2 min; when the improved Faster R-CNN iterates 8000 times, the training time is 78.7 min.

3) SHEATH BLIGHT

For sheath blight, the recognition results are reflected in Figure 19, indicating that the method put forward in this

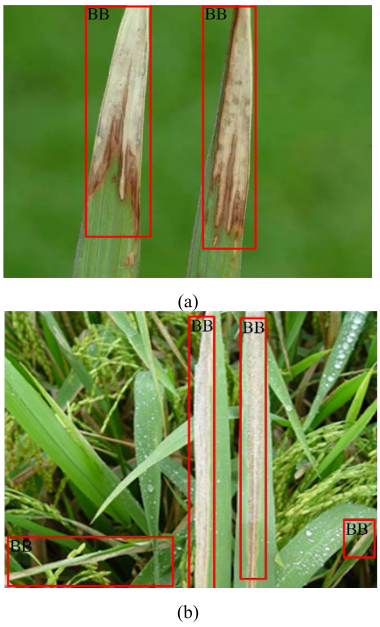

FIGURE 15. Identification of bacterial blight.

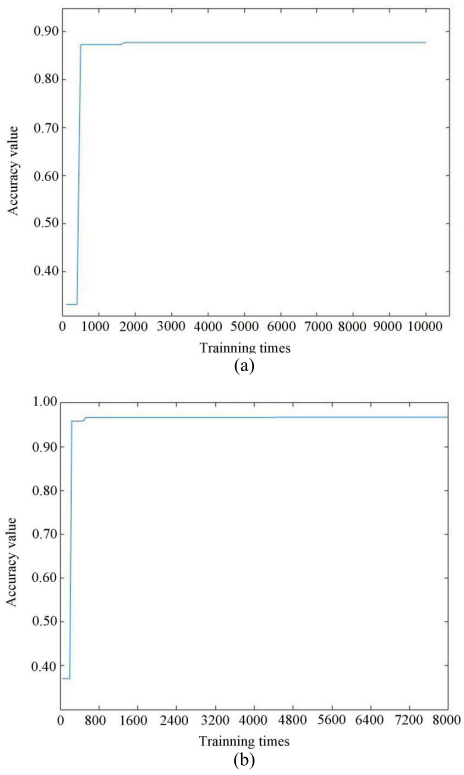

FIGURE 16. Recognition rate of bacterial leaf blight: (a) Faster R-CNN recognition rate; (b) FCM-KM + Faster R-CNN recognition rate.

paper can accurately identify the sheath blight lesions. As can be seen from Figure 20. a, the accuracy rate of Faster R-CNN reached 50.00% when trained to about 500 rounds, and the recognition accuracy of rice diseases reached 85.00% after 1200 times of training. From Figure 20. b, the accuracy

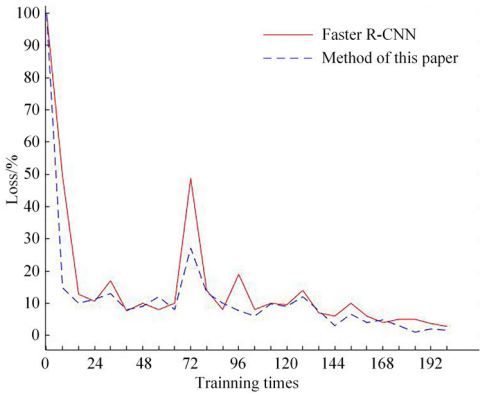

FIGURE 17. Loss function line chart for bacterial leaf blight.

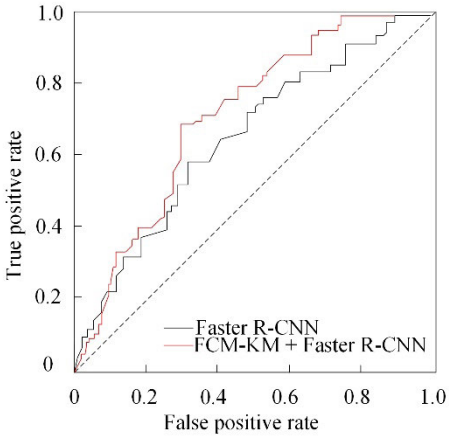

FIGURE 18. ROC curve of two algorithms about bacterial leaf blight.

TABLE 6. Comparison of different network terations and training time in sheath blight.

Faster R-CNN		FCM-KM + Faster R-CNN	
Number of iterations	Training time/min	Number of iterations	Training time/min
10000	109.7	8000	67.3

of the improved Faster R-CNN recognition is completed. After that, it reached 98.26%, and the recognition accuracy reached 50% when trained to about 200 rounds. From Fig. 21, we know that the algorithm in this paper has a lower value of the Faster R-CNN algorithm than the unimproved Faster function, and can converge to a stable state more quickly. Figure 22 shows the roc curves for the two algorithms of the rice blast data set. We can see that the Faster R-CNN curve after fusion with FCM-KM is closest to the upper left corner, indicating that its TPR is higher when its FPR is lower, which means that the detection method is more effective. According to Table 6, when the Faster R-CNN iteration is 10000 times, the training time is 109.7 min; when the improved Faster R-CNN iterates 8000 times, the training time is 67.3 min.

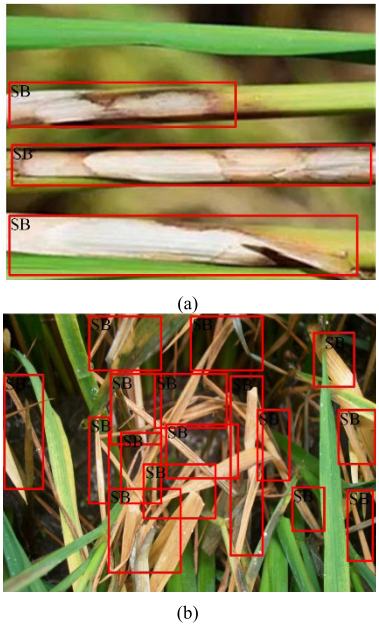

FIGURE 19. Identification of sheath blight.

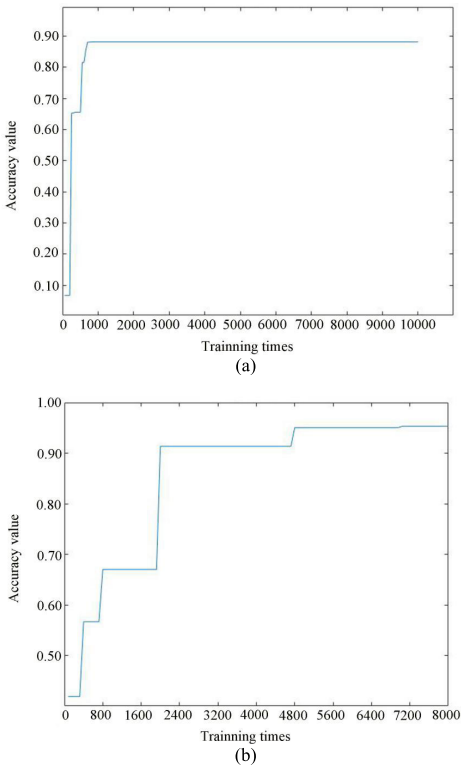

FIGURE 20. Recognition rate of sheath blight: (a) Faster R-CNN recognition rate. (b) FCM-KM + faster R-CNN recognition rate.

B. COMPARISON OF LEARNING RATES

The relationship between the running time and accuracy of the improved Faster R-CNN algorithm and the learning rate is studied by selecting different learning rates. Then, we set three different learning rates, which are 0.01, 0.001,

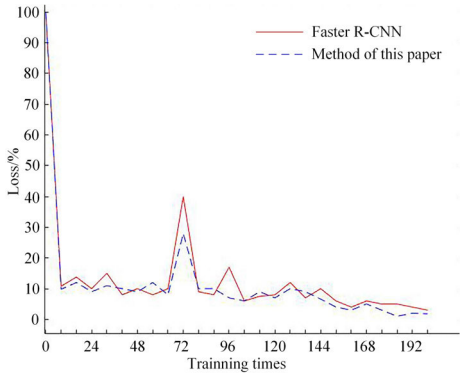

FIGURE 21. Loss function line chart for sheath blight.

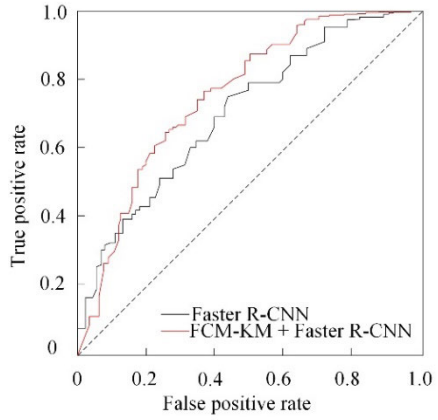

FIGURE 22. ROC curve of two algorithms about sheath blight.

TABLE 7. Comparison of experiments at different learning rates.

Learning rate	Average accuracy/%	Training time/min
0.01	90.2	55.3
0.001	97.8	76.1
0.0001	91.7	97.5

and 0.0001, respectively. In addition to the learning rate, other parameter settings are the same. Finally, we get training time and the accuracy rate under different learning rates.

After testing, the results can be found in Table 7. When the learning rate is 0.01, the time and running time of the improved Faster R-CNN algorithm are shorter, but its accuracy is not high. When the learning rate is 0.001, the improved Faster R-CNN algorithm converges slowly and runs longer. After analysis, the learning rate is large, and the training time is small, but it is difficult to guarantee accuracy; while the learning rate is small, the model is difficult to converge, and the training time is longer; by comparison, we can see that although the training time is relatively long, the accuracy is the highest, so the learning rate should be set to be 0.001.

TABLE 8. Comparison of test performance of different algorithms.

	FCM-KM + Faster R-CNN		Faster R-CNN	
	Accuracy of recognition /%	Speed of recognition /s	Accuracy of recognition /%	Speed of recognition /s
Rice blast	96.71	0.45	92.32	3.17
Bacterial blight	97.53	0.62	91.89	3.24
Sheath blight	98.26	0.43	89.64	4.75

TABLE 9. Comparison of recognition rates of different algorithms.

Algorithm	Algorithm in this text	[4]	[12]	[15]	[17]
Recognition rate/%	97.2	82	87.9	92.5/ 87.5	92

C. OVERALL PERFORMANCE COMPARISON

We compared the results of the fusion of FCM-KM with Faster R-CNN with the results of only using Faster R-CNN. Table 8 presents the performance of the methods. The detection accuracy and time of the fusion of FCM-KM with Faster R-CNN algorithm for the rice blast, bacterial blight, and sheath blight were 96.71%/0.45s, 97.53%/0.62s, and 98.26%/0.43s, respectively; Faster R-CNN detection accuracy and time are 92..32%/3.17s, 91.89%/3.24s, and 89.64%/4.75s, respectively. And the fusion of FCM-KM with Faster R-CNN algorithm has an average accuracy of 6.21% and an average time increase of 3.22s. Based on the above results, the combination of FCM-KM and Faster R-CNN algorithm is superior to the traditional Faster R-CNN algorithm in the speed and accuracy of rice disease recognition. This is because K-Means improved by firefly algorithm, chaos theory and maximum minimum distance algorithm has better performance. It avoids falling into local optimum and overcomes the difficulty of choosing K values. It is fused with the Faster R-CNN algorithm to determine the enclosing and size according to the target size in the data set, thereby improving the convergence speed and detection accuracy.

In addition, this paper also compares the recognition rates of algorithms in other literature, as shown in Table 9. For articles with two or more diseases, this article takes the average recognition rate. It can be seen that the algorithm

has better recognition effect and higher recognition rate than other algorithms.

V. CONCLUSION

With the development of technology of computer and machine vision advance, experts and scholars both at home and abroad have conducted extensive research on into the image analysis technology. In the most recent years, have witnessed the increasingly widespread application of leaf lesion identification based on deep learning has been increasingly applied to the detection of crop diseases. In this paper, a rice disease image database is established for the fast detection of rice blast, bacterial blight, and blight, with 2DFM-AMMF noise reduction and Faster 2D-Otsu segmentation used. The final average accuracy rate is 97.2%.

At present, the research conducted into threshold segmentation algorithm has been highly extensive, with many scholars improving and expanding it and to achieve some desirable outcomes.

The Faster 2D-Otsu algorithm referred to in this paper has achieved excellent results in the application of segmentation of rice disease images. Besides, it has shown the capability to eliminate most of the background interference including rice ear and disease-free rice leaves, despite some rice ears that remain. Therefore, a further investigation is conducted into the application of threshold segmentation theory in the segmentation of plant leaf diseases for the sake of ensuring that the diseased parts of the picture are completely segmented with other interference being minimized, which is one of the next priorities for the following works.

In addition, the automated rice disease detection has yet to be widely applied, and no thorough study has been performed on the real-time dynamic detection of rice diseases. A large majority of the existing methods of disease detection are focused on the detection of collected pictures.

The method proposed in this paper also identifies diseases by monitoring the collected pictures, which makes it not suited to monitoring large-scale rice cultivation at present. Therefore, in the future, further investigation shall be conducted into how to apply this method to the dynamic detection of large-scale rice planting detection and disease. For the future, in the process of popularizing this method, there is a necessity to combine intelligent Internet facilities such as agricultural Internet of Things and mobile terminal processor to realize real-time monitoring and pest identification of grain storage warehouses, which is conducive to promoting the modernization and intelligence of the agricultural industry.

REFERENCES

[1] C. Niu, Y. Li, and H. Li, "Strawberry pest identification based on image gray histogram," *Jiangsu Agricult. Sci.*, vol. 45, no. 4, pp. 169–171, 2017.

[2] Y. Xiang, "Prevention and control of common rice diseases," *Rural Economy Technol.*, vol. 29, no. 16, p. 25, 2018.

[3] Y. Yu, "Identification and prevention of common pests and diseases in rice," *Plant Protection*, vol. 61, no. 22, p. 61, 2018.

[4] S. Phadikar and J. Sil, "Rice disease identification using pattern recognition techniques," in *Proc. 11th Int. Conf. Comput. Inf. Technol.*, Dec. 2008, pp. 420–423.

[5] H. Hwang and R. Haddad, "Adaptive median filters: New algorithms and results," *IEEE Trans. Image Process.*, vol. 4, no. 4, pp. 499–502, Apr. 1995. doi: 10.1109/83.370679.

[6] X. E. Pantazi, D. Moshou, A. A. Tamouridou, "Automated leaf disease detection in different crop species through image features analysis and one class classifiers," *Comput. Electron. Agricult.*, vol. 156, pp. 96–104, Jan. 2018. doi: 10.1016/j.compag.2018.11.005.

[7] M. Rahnemoonfar and C. Sheppard, "Deep count: Fruit counting based on deep simulated learning," *Sensors*, vol. 17, no. 4, p. 905, Apr. 2017. doi: 10.3390/s17040905.

[8] S. Zhang, S. Zhang, C. Zhang, X. Wang, and Y. Shi, "Cucumber leaf disease identification with global pooling dilated convolutional neural network," *Comput. Electron. Agricult.*, vol. 162, pp. 422–430, Jul. 2019. doi: 10.1016/j.compag.2019.03.012.

[9] J. Ma, K. Du, F. Zheng, L. Zhang, Z. Gong, and Z. Sun, "A recognition method for cucumber diseases using leaf symptom images based on deep convolutional neural network," *Comput. Electron. Agricult.*, vol. 154, pp. 18–24, Nov. 2018. doi: 10.1016/j.compag.2018.08.048.

[10] X. Zhang, Y. Qiao, F. Meng, C. Fan, and M. Zhang, "Identification of maize leaf diseases using improved deep convolutional neural networks," *IEEE Access*, vol. 6, pp. 30370–30377, 2018. doi: 10.1109/ACCESS.2018.2844405.

[11] F. Qin, D. Liu, B. Sun, L. Ruan, Z. Ma, and H. Wang, "Identification of alfalfa leaf diseases using image recognition technology," *PLoS ONE*, vol. 11, no. 12, 2016, Art. no. e0168274. doi: 10.1371/journal.pone.0168274.

[12] C.-L. Chung, K.-J. Huang, S.-Y. Chen, M.-H. Lai, Y.-C. Chen, and Y.-F. Kuo, "Detecting Bakanae disease in rice seedlings by machine vision," *Comput. Electron. Agricult.*, vol. 121, pp. 404–411, Feb. 2016. doi: 10.1016/j.compag.2016.01.008.

[13] Y. Lu, S. Yi, N. Zeng, Y. Liu, and Y. Zhang, "Identification of rice diseases using deep convolutional neural networks," *Neurocomputing*, vol. 267, pp. 378–384, Dec. 2017.

[14] C. R. Rahman, P. S. Arko, M. E. Ali, M. A. I. Khan, A. Wasif, S. H. Apon, and F. Nowrin, "Identification and recognition of rice diseases and pests using convolutional neural networks," 2018, *arXiv:1812.01043*. [Online]. Available: https://arxiv.org/abs/1812.01043

[15] B. S. Ghyar and G. K. Birajdar, "Computer vision based approach to detect rice leaf diseases using texture and color descriptors," in *Proc. Int. Conf. Inventive Comput. Inform. (ICICI)*, Nov. 2017, pp. 1074–1078.

[16] H. Huang, J. Deng, Y. Lan, A. Yang, L. Zhang, S. Wen, H. Zhang, Y. Zhang, and Y. Deng, "Detection of helminthosporium leaf blotch disease based on UAV imagery," *Appl. Sci.*, vol. 9, no. 3, p. 558, 2019. doi: 10.3390/app9030558.

[17] S. Huang, C. Sun, and L. Qi, "Rice ear blast detection method based on deep convolutional neural network," *Trans. Chin. Soc. Agricult. Eng.*, vol. 33, no. 20, pp. 169–175, 2017.

[18] W.-J. Liang, H. Zhang, G.-F. Zhang, and H.-X. Cao, "Rice blast disease recognition using a deep convolutional neural network," *Sci. Rep.*, vol. 9, no. 1, 2019, Art. no. 2869. doi: 10.1038/s41598-019-38966-0.

[19] K. Bashir, M. Rehman, and M. Bari, "Detection and classification of rice diseases: An automated approach using textural features," *Mehran Univ. Eng. Eng. Eng. Technol.*, vol. 38, no. 1, pp. 239–250, 2019. [Online]. Available: http://www.publications.muet.edu.pk/index.php/muetrj/article/view/759/310

[20] Q. Yao, Z. Guan, Y. Zhou, J. Tang, Y. Hu, and B. Yang, "Application of support vector machine for detecting rice diseases using shape and color texture features," in *Proc. Int. Conf. Eng. Comput.*, Hong Kong, May 2009, pp. 79–83. doi: 10.1109/ICEC.2009.73.

[21] S. Ren, K. He, R. Girshick, and J. Sun, "Faster R-CNN: Towards real-time object detection with region proposal networks," *IEEE Trans. Pattern Anal. Mach. Intell.*, vol. 39, no. 6, pp. 1137–1149, Jun. 2017. doi: 10.1109/tpami.2016.2577031.

[22] B.-G. Wei, "Improved adaptive median filtering," *J. Comput. Appl.*, vol. 28, no. 7, pp. 1732–1734, 2008. doi: 10.3724/sp.j.1087.2008.01732.

[23] J. Ma and L. Li, "A registration algorithm based on feature point," in *Proc. Int. Conf. Inf. Technol. Comput. Eng. Manage. Sci.*, Sep. 2011, pp. 320–323.

[24] Y. Hu and H. Ji, "Research on image median filtering algorithm and its FPGA implementation," in *Proc. WRI Global Congr. Intell. Syst.*, May 2009, pp. 226–230.

[25] X. Li, "Research on image threshold segmentation algorithm based on MATLAB," *Softw. Guide*, vol. 13, no. 12, pp. 76–78, 2014.

[26] J. Zhong and H. Wu, "Evolutionary game algorithm for image segmentation," *J. Electr. Comput. Eng.*, vol. 2017, Jul. 2017, Art. no. 8746010. doi: 10.1155/2017/8746010.
[27] C. L. Chowdhary, G. V. K. Sai, D. P. Acharjya, "Decrease in false assumption for detection using digital mammography," in *Computational Intelligence in Data Mining—Volume 2* (Advances in Intelligent Systems and Computing), vol. 411, H. Behera and D. Mohapatra, eds. New Delhi, India: Springer, 2016.
[28] Y. Guo, P. Su, and Y. Wu, "Robot target detection and spatial localization based on faster R-CNN," *J. Huazhong Univ. Sci. Technol. (Natural Sci. Ed.)*, vol. 46, no. 12, pp. 55–59, 2018.
[29] R. Girshick, J. Donahue, T. Darrell, and J. Malik, "Rich feature hierarchies for accurate object detection and semantic segmentation," in *Proc. IEEE Conf. Comput. Vis. Pattern Recognit.*, Columbus, OH, USA, Jun. 2014, pp. 580–587. doi: 10.1109/CVPR.2014.81.
[30] R. Girshick, "Fast R-CNN," in *Proc. IEEE Int. Conf. Comput. Vis. (ICCV)*, Santiago, Chile, Dec. 2015, pp. 1440–1448. doi: 10.1109/ICCV.2015.169.
[31] R. Girshick, J. Donahue, T. Darrell, and J. Malik, "Region-based convolutional networks for accurate object detection and segmentation," *IEEE Trans. Pattern Anal. Mach. Intell.*, vol. 38, no. 1, pp. 142–158, Jan. 2016. doi: 10.1109/tpami.2015.2437384.
[32] L. Ramaswamy, B. Carminati, J. B. D. Joshi, and C. Pu, "Editorial: Collaborative computing: Networking, applications and worksharing (CollaborateCom 2012)," *Mobile Netw. Appl.*, vol. 19, no. 5, p. 634, Oct. 2014. doi: 10.1007/s11036-014-0532-9.
[33] W.-J. Chang, L.-B. Chen, C.-H. Hsu, C.-P. Lin, and T.-C. Yang, "A deep learning-based intelligent medicine recognition system for chronic patients," *IEEE Access*, vol. 7, pp. 44441–44458, 2019. doi: 10.1109/access.2019.2908843.
[34] D. Pandian, *Proceedings of the International Conference on ISMAC in Computational Vision and Bio-Engineering 2018 (ISMAC-CVB)*. Palladam, India: SCAD Institute of Technology, 2019.
[35] *Data Science*. Springer, 2018.
[36] M. Yang, C. Ma, and Y. Wang, "A FCMM algorithm for improving K-means clustering," *Appl. Res. Comput.*, vol. 36, no. 7, pp. 2007–2010, Sep. 2019. doi: 10.3969/j.issn.1001-3695.2017.12.0851.
[37] J. Wang, N. Mao, X. Chen, J. Ni, C. Wang, and Y. Q. Shi, "Multiple histograms based reversible data hiding by using FCM clustering," *Signal Process.*, vol. 159, pp. 193–203, Jun. 2019. doi: 10.1016/j.sigpro.2019.02.013.
[38] M. Chen, C. Tang, M. Xu, and Z. Lei, "A clustering framework based on FCM and texture features for denoising ESPI fringe patterns with variable density," *Opt. Lasers Eng.*, vol. 119, pp. 77–86, Aug. 2019. doi: 10.1016/j.optlaseng.2019.03.015.
[39] S. J. Peng, C. C. Lee, H. M. Wu, C. J. Lin, C. Y. Shiau, W. Y. Guo, D. H. C. Pan, K. D. Liu, W. Y. Chung, and H. C. Yang, "Fully automated tissue segmentation of the prescription isodose region delineated through the gamma knife plan for cerebral arteriovenous malformation (AVM) using fuzzy C-means (FCM) clustering," *NeuroImage, Clinical*, vol. 21, Jan. 2019, Art. no. 101608. doi: 10.1016/j.nicl.2018.11.018.
[40] C. L. Chowdhary and D. P. Acharjya, "Breast cancer detection using intuitionistic fuzzy histogram hyperbolization and possibilitic fuzzy c-mean clustering algorithms with texture feature based classification on mammography images," in *Proc. Int. Conf. Adv. Inf. Commun. Technol. Comput.*, Aug. 2016, Art. no. 21.
[41] C. L. Chowdhary and D. P. Acharjya, "Clustering algorithm in possibilistic exponential fuzzy C-mean segmenting medical images," *J. Biomimetics, Biomater. Biomed. Eng.*, vol. 30, pp. 12–23, Jan. 2017. doi: 10.4028/www.scientific.net/jbbbe.30.12.
[42] A. H. Gandomi, X-S. Yang, S. Talatahari, and A. H. Alavi, "Firefly algorithm with chaos," *Commun. Nonlinear Sci. Numer. Simul.*, vol. 18, no. 1, pp. 89–98, Jan. 2013. doi: 10.1016/j.cnsns.2012.06.009.
[43] Y. He, J. Zhou, C. Li, J. Yang, and Q. Li, "A precise chaotic particle swarm optimization algorithm based on improved tent map," in *Proc. 4th Int. Conf. Natural Comput.*, Jinan, China, Oct. 2008, pp. 569–573. doi: 10.1109/ICNC.2008.588.
[44] N. Zeng, Z. Wang, B. Zineddin, Y. Li, M. Du, L. Xiao, X. Liu, and T. Young, "Image-based quantitative analysis of gold immunochromatographic strip via cellular neural network approach," *IEEE Trans. Med. Imag.*, vol. 33, no. 5, pp. 1129–1136, May 2014. doi: 10.1109/tmi.2014.2305394.
[45] N. Zeng, Z. Wang, H. Zhang, W. Liu, and F. E. Alsaadi, "Deep belief networks for quantitative analysis of a gold immunochromatographic strip," *Cognit. Comput.*, vol. 8, no. 4, pp. 684–692, 2016. doi: 10.1007/s12559-016-9404-x.
[46] N. Zeng, H. Zhang, Y. Li, J. Liang, and A. M. Dobaie, "Denoising and deblurring gold immunochromatographic strip images via gradient projection algorithms," *Neurocomputing*, vol. 247, pp. 165–172, Jul. 2017. doi: 10.1016/j.neucom.2017.03.056
[47] Y. LeCun, Y. Bengio, and G. Hinton, "Deep learning," *Nature*, vol. 521, pp. 436–444, May 2015. doi: 10.1038/nature14539.
[48] N. Zeng, H. Li, Y. Li, and X. Luo, "Quantitative analysis of immunochromatographic strip based on convolutional neural network," *IEEE Access*, vol. 7, pp. 16257–16263, 2019. doi: 10.1109/access.2019.2893927.

GUOXIONG ZHOU received the B.Sc. degree from Hunan Agricultural University, in 2002, and the M.Sc. and Ph.D. degrees from Central South University, in 2006 and 2010, respectively. He is currently an Associate Professor with the Central South University of Forestry and Technology. His main research interests include forest fire prevention and robots.

WENZHUO ZHANG was born in 1996. He received the bachelor's degree from the Central South University of Forestry and Technology. His main research directions of postgraduate study are forest fire prevention and graphic image processing.

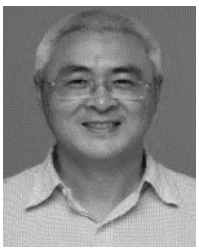

AIBIN CHEN was born in Hunan, China, in 1971. He is currently pursuing the Ph.D. degree. He has served as a professor. His research direction is image processing.

MINGFANG HE was born in 1985. She received the Ph.D. degree. Her main research interests include control science and engineering, and artificial intelligence.

XUESHUO MA studied at the Central South University of Forestry and Technology, in 2016. She is mainly involved in the studies of deep learning and image processing.